

Contribution of real-time elastography in diagnosis of polycystic ovary syndrome

Saliha Çıracı, Sinan Tan, Ayşenur Şirin Özcan, Ahmet Aslan, Hüseyin Levent Keskin, Ömer Faruk Ateş, Yıldız Akçay, Halil Arslan

PURPOSE

We aimed to assess the feasibility and reproducibility of real-time elastography (RTE) for displaying the effects of morphological changes in the ovary in polycystic ovary syndrome (PCOS).

METHODS

Forty-eight patients diagnosed with PCOS and 48 healthy women were enrolled in the study. Ultrasonography and RTE were performed on the 3rd day of the menstrual cycle. Evaluations were performed independently by two radiologists. Ovarian volume, number of follicles, elasticity pattern, and strain ratio were measured. Elasticity patterns were assessed as hard (type 1; blue or blue-green), moderate (type 2; green or green-yellow) or soft (type 3; red or orange-red).

RESULTS

Both radiologists determined the elasticity pattern as mostly type 1 in the PCOS group and type 3 in the control group ($P < 0.01$). The mean strain ratios obtained by the first and second radiologist were 6.1 ± 1.8 (2.7–10.1) and 6.0 ± 1.5 (3.0–9.0) in PCOS and 3.3 ± 1.2 (1.7–7.2) and 3.2 ± 0.9 (1.7–6.8) in the control group, respectively ($P < 0.001$). Interobserver agreement was moderate for the elasticity pattern ($\kappa=0.48$) and good for the strain ratio (intraclass correlation coefficient, 0.77). A strain ratio of 3.8 was determined as the optimized cutoff point by receiver operating curve analysis. Strain ratio was correlated with the ovarian volume and the number of detected follicles ($P < 0.001$).

CONCLUSION

Elasticity pattern and strain ratio can help identify morphological changes that make PCOS ovaries stiffer than normal ovaries.

In reproductive-aged women, polycystic ovary syndrome (PCOS) is an important cause of infertility and is characterized by menstrual irregularities, hirsutism and signs of hyperandrogenism, and polycystic ovary appearance (1–3). In addition to insulin resistance, serum androgenic hormone levels are increased, causing undesired effects on women's metabolic, reproductive, and cardiovascular health (1–5). PCOS is characterized by enlarged ovaries containing small cysts, for which the syndrome was named (6).

Real-time elastography (RTE) is a novel and dynamic imaging technique that is simply based on the hardness or softness of tissues or organs under the appropriate compression and can be used with conventional ultrasonography (US) probes after performing gray-scale and Doppler US. Displacement of soft tissues is greater than hard tissues, and tissue hardness is displayed as a color-coded image that lays over the gray-scale US image translucently (7). Elastography has been used previously for differentiation of pathologies of tissues and organs, such as thyroid, breast, kidneys, and liver (7–9). There are limited studies about the elastographic properties of the ovaries, mostly focused on ovarian neoplasms and, to the best of our knowledge, there is no medical data concerning the elasticity properties of the ovary in PCOS (10, 11). In this study, our purpose was to assess the feasibility and reproducibility of RTE for displaying the effects of morphological changes in the ovary in PCOS and to put forward the value of RTE as a new diagnostic approach for diagnosing PCOS.

Methods

Patients

This observational study was approved by the institutional review board and informed written consent was obtained from all reviewed subjects.

Forty-eight patients who were diagnosed as PCOS by the Gynecology Department and 48 healthy women from consecutive patients who were referred to the Gynecology Department for routine control were included in the study. PCOS diagnoses were made according to the Rotterdam (ESHRE/ASRM) criteria (1, 12). The patients who had a diagnosis of Cushing syndrome, congenital adrenal hyperplasia, hyperprolactinemia, thyroid dysfunction, virilizing tumors, type 2 diabetes mellitus, or patients on medication such as oral contraceptives, glucocorticoids, antiandrogens, insulin sensitizers, or drugs that may cause hirsutism were excluded from the study. Patients who had follicles larger than 9 mm or corpus luteum cysts were also excluded because these features could potentially alter the results.

From the Department of Radiology (S.Ç., A.Ş.Ö., Ö.F.A., Y.A., H.A.), Ankara Training and Research Hospital, Ankara, Turkey; the Department of Radiology (S.T. ✉ drsinantan@gmail.com, A.A.), Bursa Şevket Yılmaz Training and Research Hospital, Bursa, Turkey; the Department of Obstetrics and Gynecology (H.L.K.), Ankara Atatürk Training and Research Hospital, Ankara, Turkey.

Received 27 February 2014, revision requested 20 March 2014, final revision received 31 August 2014, accepted 3 September 2014.

Published online 23 January 2015.
DOI 10.5152/dir.2014.14094

Presented as an oral presentation at the 20th European Symposium on Urogenital Radiology.

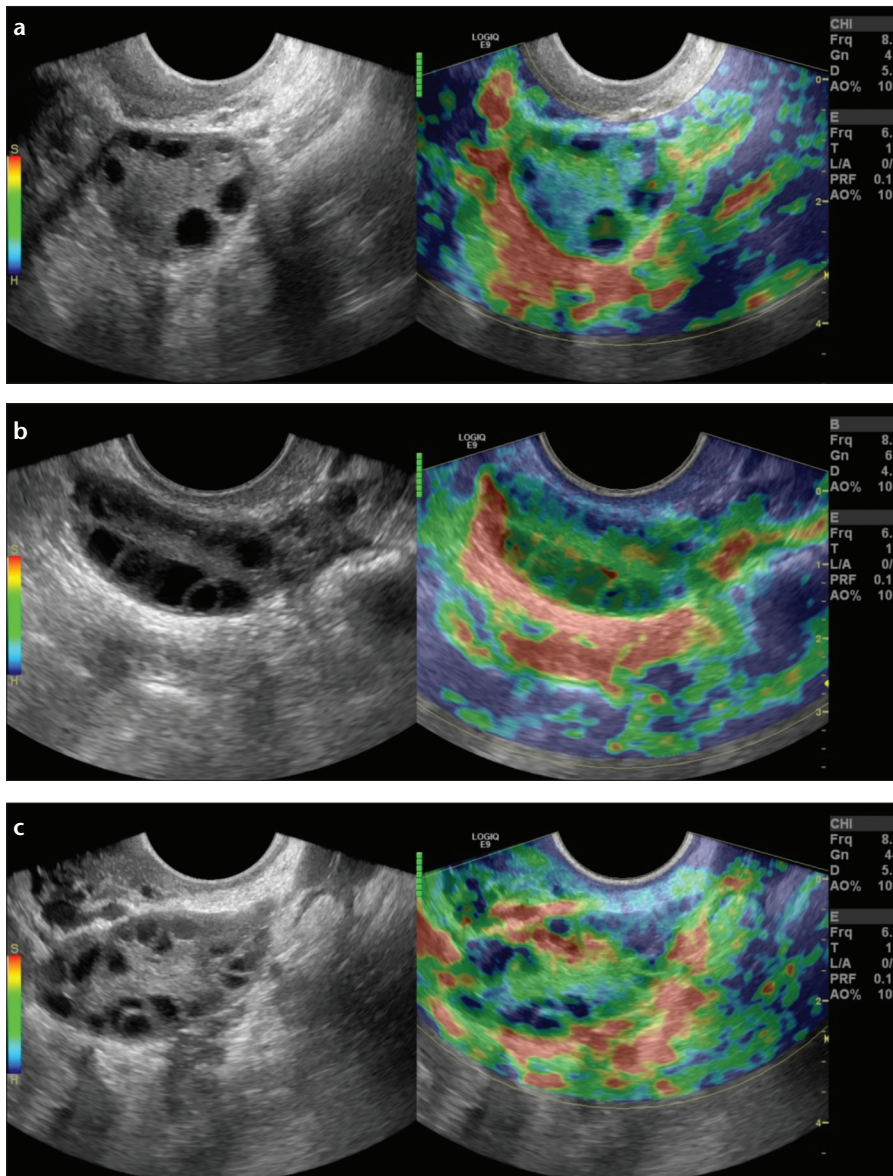


Figure 1. a–c. Gray-scale (left) and color (right) sonograms representing type 1 elasticity pattern (blue-green, a), type 2 elasticity pattern (green-yellow, b) and type 3 elasticity pattern (orange-red, c) in ovarian stroma.

Scanning and equipment

The gray-scale US and RTE studies were done using a 6.5 MHz vaginal probe (Logiq E9, GE Healthcare) on the 3rd day of the menstrual cycle by one of two radiologists having 3–5 years of experience with sonography and one year of experience in elastography, who were blinded to the patients' diagnosis, clinical features, or complaints. All transvaginal US studies were performed in a gynecologic position, when the bladder was empty.

The ovaries were examined by gray-scale US and maximum diameters in three planes (longitudinal, ante-

ro-posterior and transverse) were measured to calculate the ovarian volume by the prolate ellipsoid formula ($V = D1 \times D2 \times D3 \times 0.523 \text{ cm}^3$). The number and maximum diameter of detected follicles were noted. Scanning of ovaries was completed when each ovary was scanned from medial to lateral aspects.

RTE was performed with the same probe used in gray-scale US evaluation. Manual light compression and decompression of the ovaries by the transducer was performed attentively to achieve an optimal and consistent color coding. The quality factor of compression applied to the ovary, represented on

a bar scale of 1–7, was used to select the optimal image, and images having an adequate compression (bar scale of 5–7) were evaluated. The scanning protocol was completed after the ovarian stroma was imaged adequately. RTE and B-mode US images were simultaneously displayed as a two-panel image. The elastographic box contained the ovary, the fallopian tube, and the surrounding tissue for all patients. The elastogram was visualized on a color scale with type 1 appearing as blue or blue-green (hardest tissue, no strain), type 2 as green or green-yellow (intermediate tissue, average strain), and type 3 as red or orange-red (softest tissue, greatest strain) over the B-mode US image (Fig. 1) (13). Cine RTE images (at least five seconds per ovary) were recorded by the sonography device digitally for later evaluation.

Data analysis

After obtaining all elastograms, static images and video sequences of patients and the control group were evaluated individually by two radiologists who were blinded to the clinical and biochemical findings and final diagnoses. Elasticity patterns were assessed as hard (type 1), moderate (type 2) or soft (type 3). The strain ratio for the ovarian stroma was then calculated by comparing the stroma (A) to the adjacent soft tissue outside the ovary that was clearly not bowel or blood vessel (B). The first region-of-interest (ROI) was placed on the adjacent soft tissue (B) and the second ROI was placed on the ovary containing ovarian stroma (A) entirely (Fig. 2). The strain ratio (B/A), represented graphically, indicating the stiffness of the ovarian stroma was then calculated automatically by the sonoelastography device. A minimum of three measurements were derived for each ovary and the mean value of six measurements was used to assess the strain ratio of the ovarian stroma for each patient.

Statistical analysis

Data analysis was performed using the Statistical Package for Social Sciences (SPSS version 15.0, SPSS Inc.). Categorical variables are presented as numbers and percentages. The Kolm-

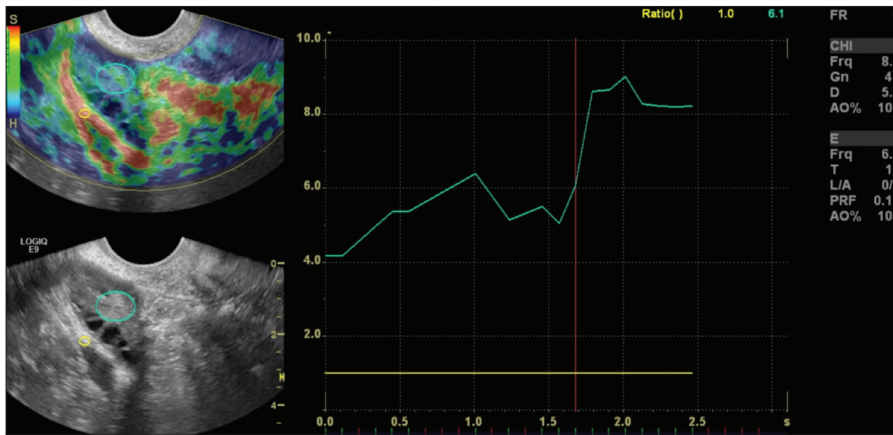


Figure 2. Elastography image of a 24-year-old woman with PCOS and graphical representation of the strain ratio. The first region-of-interest (ROI) (A, small circle) was placed in the fallopian tube and the second ROI (B, large circle) was placed in the ovarian stroma. Strain ratio was calculated automatically as B/A. The x-axis represents time in seconds; y-axis represents strain.

Table 1. Strain ratios and elasticity pattern of ovaries in PCOS and control groups by two radiologists

	Elasticity pattern				Strain ratio	
	Type 1	Type 2	Type 3	P	Mean±SD	P
Observer 1						
PCOS group	61 (63.5)	12 (12.5)	23 (23.9)	<0.001	6.1±1.8	<0.001
Control group	9 (9.3)	16 (16.6)	71 (73.9)		3.3±1.2	
Observer 2						
PCOS group	38 (39.6)	31 (32.3)	27 (28.1)	<0.001	6.0±1.5	<0.001
Control group	2 (2.1)	34 (35.4)	60 (62.5)		3.2±0.9	

Unless otherwise noted, data are presented as n (%). PCOS, polycystic ovary syndrome; SD, standard deviation.

ogorov-Smirnov test was used for testing normality of the distribution. Continuous variables with normal distribution are presented as mean±SD.

To determine interobserver agreement, the intraclass correlation coefficient (ICC) was used for the strain ratio and a weighted Cohen's kappa coefficient (κ) was used for elasticity patterns with a confidence interval (CI) of 95%, where 1.0 indicated perfect agreement and 0 indicated a chance agreement. The Student t test was used for comparison of strain ratios and chi-square test was used for comparison of elasticity patterns between groups. The Pearson correlation coefficient was used for evaluating the correlation of strain ratio with US findings of ovaries. Receiver operating characteristic (ROC) curve analysis was performed to evaluate strain ratio values

in patients with and without PCOS, and Youden's index (J) was used to determine the optimal cutoff points for the presence of PCOS, giving the same weight to sensitivity and specificity (14).

Correlation coefficients of 0.2–0.4 were accepted as weak, 0.4–0.7 as moderate, and >0.7 as strong correlations. Statistical significance was set as $P < 0.05$ and was bidirectional.

Results

The study included 48 patients diagnosed with PCOS (mean age, 25.7±4.2 years; range, 19–36 years) and 48 healthy women (mean age, 27.1±5.2 years; range, 20–38 years ($P = 0.092$)). Patients with PCOS had significantly larger mean ovarian volume (12.6±4.1 cm³ vs. 5.4±1.8 cm³, $P < 0.001$) and increased number of follicles (18.8±5.6

vs. 8.4±2.9, $P < 0.001$) than the control group.

For both observers, elasticity pattern was mostly type 1 in the PCOS group and type 3 in the control group ($P < 0.001$) (Table 1). The mean strain ratios obtained by the first and second observer were 6.1±1.8 (2.7–10.1), and 6.0±1.5 (3.0–9.0) in the PCOS group and 3.3±1.2 (1.7–7.2) and 3.2±0.9 (1.7–6.8) in the control group, respectively. Both observers measured higher strain ratios in PCOS than in the control group ($P < 0.001$) (Table 1).

The optimal cutoff for strain ratio was 3.8 ($J=0.72$ for both observers) to discriminate PCOS patients and healthy women. Diagnostic sensitivity, specificity, positive predictive value (PPV) and negative predictive value (NPV) for strain ratio, number of detected follicles, and ovarian volume are presented in Table 2.

Interobserver agreement was moderate for the elasticity pattern ($\kappa=0.48$) and good for the strain ratio (ICC=0.77; $P < 0.001$, for both parameters).

Positive moderate correlations were detected between the strain ratio and the ovarian volume ($r=0.559$, $P < 0.001$ for Observer 1; $r=0.602$, $P < 0.001$ for Observer 2), and between the strain ratio and the number of detected follicles ($r=0.553$, $P < 0.001$ for Observer 1; $r=0.636$, $P < 0.001$ for Observer 2) in PCOS and control groups.

Discussion

In this study we assessed the use of RTE for differentiating ovaries in patients with PCOS and healthy women. We determined that elasticity pattern and strain ratio parameter could be used to show the morphological changes in PCOS with moderate and good interobserver agreement, respectively.

Insulin resistance and hyperinsulinemia, exaggerated frequency and amplitude of serum luteinizing hormone secretion, increased production of ovarian and/or adrenal androgens, changes of cortisol metabolism and genetic transition can be seen in patients with PCOS (3, 15). Hyperinsulinemia, elevated serum luteinizing hormone/follicle stimulating hormone ratio, and excess androgen synthesis affect ovaries (3, 16). The luteinized and in-

Table 2. Comparison of strain ratio and gray-scale US findings to determine the presence of PCOS

Parameters	Strain ratio				US findings			
	Observer 1	<i>P</i>	Observer 2	<i>P</i>	No. of follicles	<i>P</i>	Ovarian volume (cm ³)	<i>P</i>
AUC	0.888	<0.001	0.939	<0.001	0.959	<0.001	0.962	<0.001
Optimal cutoff	>3.8		>3.8		≥12		≥10	
Sensitivity (%)	87.50		89.5		85.4		100	
Specificity (%)	85.42		83.3		89.5		70.8	
PPV (%)	85.7		84.3		89.1		77.4	
NPV (%)	87.2		88.8		86		100	

US, ultrasonography; PCOS, polycystic ovary syndrome; AUC, area under the curve; PPV, positive predictive value; NPV, negative predictive value.

creased numbers of stromal theca cells around the follicles disrupt the maturation of follicles and are related to increased ovarian volume. Increased ovarian volume and number of thecal cells in the ovarian stroma, and thick fibrotic albuginea make the ovary harder than normal, which can be demonstrated by RTE (17).

There are different classifications of elasticity patterns with RTE. In the current study we used three types of elasticity patterns for assessing ovarian stiffness, which we thought easy to use (13). The type 1 pattern indicates hard tissue with no or little elasticity, while type 3 indicates a soft tissue with high elasticity. Both observers agreed that ovaries in PCOS were significantly harder than those of the control group. The discrepancy between the two observers in type 1 and type 2 elasticity patterns for both study and control groups was reasonable and the interobserver agreement was moderate ($\kappa=0.48$). However, our findings require a simple and adequate classification of elasticity patterns for assessing ovarian stiffness. Also, evaluating the elasticity pattern on elastographic color images requires experience and makes the evaluation subjective.

We analyzed the strain ratio of the ovarian stroma, which we thought to be more objective than the elasticity pattern, because it showed images of relative tissue hardness (18). The strain ratio is a semiquantitative measurement of hardness of the lesion with respect to the adjacent soft tissues, where higher ratios point to harder

tissues (9). We displayed the adjacent soft tissue in elastographic images and used it for comparison, to achieve a strain ratio. We detected high strain ratios in PCOS, representing the hard ovarian stroma, and found substantial interobserver agreement ($ICC=0.77$), which supports our theory. We chose a cutoff value of 3.8 for discrimination between the PCOS and control groups by strain ratio, which was closer to the mean strain ratio of the control group than the mean strain ratio of the PCOS group. We obtained sensitivity, specificity, PPV, and NPV values similar to those obtained from US findings of PCOS, such as detected number of follicles and ovarian volume. Although we did not compare patients with polycystic ovaries and PCOS patients without polycystic ovary appearance, this may imply that RTE, by providing the quality factor of compression, can be a useful diagnostic tool compared to the time consuming counting of ovarian follicles or ovarian volume by gray-scale US (10). Also RTE displays ovarian stiffness as a result of histopathological changes in ovaries due to PCOS.

Both observers had false-positive or false-negative diagnoses by elasticity pattern or strain ratio, which could be related to previous diseases that affected the ovaries, such as infections, gonadal hormonal imbalances, or medications. Such previous diseases can change the elasticity properties of the ovaries and can make ovarian stroma harder or softer than normal, thus altering the RTE appearance or strain ratio of the ovaries. Also, dura-

tion of PCOS may affect the elasticity properties of the ovaries. With prolonged disease, older follicles regress, convert into stroma, and increase the subcortical stroma (15). Further studies comparing RTE with histopathological findings of the ovary and disease duration will be beneficial for solidifying this theory. Additionally, medications for PCOS may affect the ovaries, and thus, the ovarian stroma stiffness.

In this study the strain ratio showed moderate positive correlations with ovarian volume and the number of detected follicles which may be explained by a mechanism related with hyperandrogenism.

In our study, we had several limitations. First, polycystic ovary appearance can be seen in many healthy women under certain situations, such as taking combined contraceptive drugs, anovulation, and obesity (19). We did not have patients with polycystic ovary appearance in the control group and could not compare our results with them. Second, we excluded patients having cysts exceeding 9 mm, but small cysts around the ovarian stroma may affect the compression of the ovarian stroma due to the absence of strain of the fluid in them (20). Also RTE by transvaginal probe necessitates experience to evaluate the stiffness of the ovarian stroma because it requires lighter pressure rather than strong compression (10). Finally, we did not compare the strain ratio of the ovarian stromas in PCOS after various treatments, which could confirm that ovarian stiffness remains the same with PCOS.

In conclusion, this study highlights the possibility of PCOS evaluation by RTE, a relatively new, available, and dynamic imaging modality that can help to show morphological changes in PCOS. Elastographic features of ovarian stroma may have a role in the diagnosis of PCOS, like gray-scale US, especially using the strain ratio. However, further studies comparing women with polycystic ovaries with or without clinical symptoms or hormonal parameters of PCOS are needed to understand and appreciate the value of RTE in the diagnosis of PCOS.

Conflict of interest disclosure

The authors declared no conflicts of interest.

References

1. Frauser BC, Tarlatzis BC, Rebar RW, et al. Consensus on women's health aspects of polycystic ovary syndrome (PCOS): the Amsterdam ESHRE/ASRM-sponsored 3rd PCOS Consensus Workshop Group. *Fertil Steril* 2012; 97:28–38. [\[CrossRef\]](#)
2. Azziz R, Marin C, Hoq L, Badamgarav E, Song P. Health care-related economic burden of the polycystic ovary syndrome during the reproductive life span. *J Clin Endocrinol Metab* 2005; 90:4650–4658. [\[CrossRef\]](#)
3. Ehrmann DA. Polycystic ovary syndrome. *N Engl J Med* 2005; 352:1223–1236. [\[CrossRef\]](#)
4. Sattar N. PCOS, insulin resistance and long-term risks for diabetes and vascular disease. *Br J Diabetes Vasc Dis* 2009; 9:15–18. [\[CrossRef\]](#)
5. Fraser IS, Kovacs G. Current recommendations for the diagnostic evaluation and follow-up of patients presenting with symptomatic polycystic ovary syndrome. *Best Pract Res Clin Obstet Gynaecol* 2004; 18:813–823. [\[CrossRef\]](#)
6. Lujan ME, Chizen ME, Pierson RA. Diagnostic criteria for polycystic ovary syndrome: pitfalls and controversies. *J Obstet Gynaecol Can* 2008; 30:671–679.
7. Morikawa H, Fukuda K, Kobayashi S, et al. Real-time tissue elastography as a tool for the noninvasive assessment of liver stiffness in patients with chronic hepatitis C. *J Gastroenterol* 2011; 46:350–358. [\[CrossRef\]](#)
8. Jung HJ, Hahn SY, Choi HY, Park SH, Park HK. Breast sonographic elastography using an advanced breast tissue-specific imaging preset: initial clinical results. *J Ultrasound Med* 2012; 31:273–280.
9. Tan S, Özcan MF, Tezcan F, et al. Real-time elastography for distinguishing angiomyolipoma from renal cell carcinoma: preliminary observations. *AJR Am J Roentgenol* 2013; 200:W369–375. [\[CrossRef\]](#)
10. Ciledağ N, Arda K, Aktas E, Aribas BK. A pilot study on real-time transvaginal ultrasonographic elastography of cystic ovarian lesions. *Indian J Med Res* 2013; 137:1089–1092.
11. Onur MR, Şimşek BÇ, Kazez A. Sclerosing stromal tumor of the ovary: ultrasound elastography and MRI findings on preoperative diagnosis. *J Med Ultrasonics* 2011; 38:217–220. [\[CrossRef\]](#)
12. Rotterdam ESHRE/ASRM-Sponsored PCOS Consensus Workshop Group. Revised 2003 consensus on diagnostic criteria and long-term health risks related to polycystic ovary syndrome. *Fertil Steril* 2004; 81:19–25. [\[CrossRef\]](#)
13. Cho N, Jang M, Lyou CY, Park JS, Choi HY, Moon WK. Distinguishing benign from malignant masses at breast US: combined US elastography and color Doppler US – influence on radiologist accuracy. *Radiology* 2012; 262:80–90. [\[CrossRef\]](#)
14. Zweig MH, Campbell G. Receiver-operating characteristics (ROC) plots: a fundamental evaluation tool in clinical medicine. *Clin Chem* 1993; 39:561–577.
15. Hughesdon PE. Morphology and morphogenesis of the Stein-Leventhal ovary and of so-called “hyperthecosis”. *Obstet Gynecol Surv* 1982; 37:59–77. [\[CrossRef\]](#)
16. Tsilchorozidou T, Overton C, Conway GS. The pathophysiology of polycystic ovary syndrome. *Clin Endocrinol (Oxf)* 2004; 60:1–17. [\[CrossRef\]](#)
17. Fulghesu AM, Angioni S, Frau E, et al. Ultrasound in polycystic ovary syndrome—the measuring of ovarian stroma and relationship with circulating androgens results of a multicentric study. *Hum Reprod* 2007; 22:2501–2508. [\[CrossRef\]](#)
18. Koizumi Y, Hirooka M, Kisaka Y, et al. Liver fibrosis in patients with chronic hepatitis C: Noninvasive diagnosis by means of real-time tissue elastography—establishment of the method for measurement. *Radiology* 2011; 258:610–617. [\[CrossRef\]](#)
19. Balen AH, Laven JS, Tan SL, Dewailly D. Ultrasound assessment of the polycystic ovary: international consensus definitions. *Hum Reprod Update* 2003; 9:505–514. [\[CrossRef\]](#)
20. Moon HJ, Sung JM, Kim EK, Yoon JH, Youk JH, Kwak JY. Diagnostic performance of gray-scale US and elastography in solid thyroid nodules. *Radiology* 2012; 262:1002–1013. [\[CrossRef\]](#)